Title

Trichomonas vaginalis extracellular vesicles are internalized by host cells using proteoglycans and caveolin-dependent endocytosis

Journal

Proceedings of the National Academy of Sciences of the United States of America, 116(43)

ISSN

0027-8424

Authors

Rai, Anand Kumar
Johnson, Patricia J

Publication Date

2019-10-22

DOI

10.1073/pnas.1912356116

Peer reviewed

Trichomonas vaginalis extracellular vesicles are internalized by host cells using proteoglycans and caveolin-dependent endocytosis

Anand Kumar Rai[a] and Patricia J. Johnson[a,1]

[a]Department of Microbiology, Immunology and Molecular Genetics, University of California, Los Angeles, CA 90095

This contribution is part of the special series of Inaugural Articles by members of the National Academy of Sciences elected in 2019.

Contributed by Patricia J. Johnson, September 13, 2019 (sent for review July 18, 2019; reviewed by Amy H. Buck and Stephen L. Hajduk)

***Trichomonas vaginalis*, a human-infective parasite, causes the most prevalent nonviral sexually transmitted infection worldwide. This pathogen secretes extracellular vesicles (EVs) that mediate its interaction with host cells. Here, we have developed assays to study the interface between parasite EVs and mammalian host cells and to quantify EV internalization by mammalian cells. We show that *T. vaginalis* EVs interact with glycosaminoglycans on the surface of host cells and specifically bind to heparan sulfate (HS) present on host cell surface proteoglycans. Moreover, competition assays using HS or removal of HS from the host cell surface strongly inhibit EV uptake, directly demonstrating that HS proteoglycans facilitate EV internalization. We identified an abundant protein on the surface of *T. vaginalis* EVs, 4-α-glucanotransferase (Tv4AGT), and show using isothermal titration calorimetry that this protein binds HS. Tv4AGT also competitively inhibits EV uptake, defining it as an EV ligand critical for EV internalization. Finally, we demonstrate that *T. vaginalis* EV uptake is dependent on host cell cholesterol and caveolin-1 and that internalization proceeds via clathrin-independent, lipid raft-mediated endocytosis. These studies reveal mechanisms used to drive host:pathogen interactions and further our understanding of how EVs are internalized by target cells to allow cross-talk between different cell types.**

Trichomonas vaginalis | extracellular vesicles | glycosaminoglycans | clathrin independent | lipid raft-mediated endocytosis

Trichomonas vaginalis is a unicellular parasite responsible for the most prevalent nonviral sexually transmitted infection (STI) worldwide, trichomoniasis (1), with ∼250 million cases reported annually. More people are infected by *T. vaginalis* than any other eukaryotic pathogen, and trichomoniasis is more prevalent than all bacterial STIs combined (2). *T. vaginalis* causes vaginitis, cervicitis, urethritis, and pelvic inflammatory disease and may lead to adverse pregnancy outcomes (3, 4). Trichomoniasis also increases the risk of HIV transmission and has been correlated with increased incidence and severity of cervical and prostate cancers (5–9). *T. vaginalis* colonizes the human urogenital tract, where it remains extracellular. Factors that allow the parasite to establish and maintain an infection are poorly understood (10–13).

Toward identifying and characterizing critical processes involved in host:pathogen interactions, we previously discovered and analyzed small membrane-bound extracellular vesicles (EVs) that are secreted by the parasite. We found that *T. vaginalis* EVs deliver proteins and RNA into host cells via unknown mechanisms and modulate parasite adherence to host cells and host cell metabolism (14, 15). EVs produced by several parasites have now been described to module host cell metabolism in many ways (16–19), including the transfer of virulence factors (20), drug resistance markers (21), and microRNAs that down-regulate host cell proteins (22–24). Pathogen EVs have also been shown to affect host cell proliferation (24, 25) and neuronal metabolism (26) and to modulate host immune responses (17, 23, 24, 27–29). Additionally, mammalian EVs have been demonstrated to play critical roles in regulating cancer, immunological, and neurological responses (30–36).

The ability of EVs produced by one cell to affect a recipient cell depends on the uptake and subsequent release of EV cargo into the recipient cell. Potential mechanisms of EV uptake include clathrin-dependent endocytosis, caveolin-mediated endocytosis, phagocytosis, or micropinocytosis. Limited analyses of mammalian EV uptake by mammalian cells have been conducted (37–39). To date, no detailed quantitative analyses of the internalization of pathogen-derived EVs have been reported.

Understanding the molecular mechanism(s) mediating the interaction and internalization of *T. vaginalis* EVs by host cells is important for understanding the role of EVs in host:parasite communication. To this end, we have established biochemical assays to monitor and quantify *T. vaginalis* EV uptake by host cells. Using these assays, we have identified surface components of both the host cell and the EV involved in internalization as well as the mechanism that drives EV uptake.

Results and Discussion

Quantification of *T. vaginalis* EV Uptake by Host Cells. *T. vaginalis* produces and secretes EVs with physical and biochemical properties similar to mammalian EVs (14, 15, 27). We previously demonstrated that EVs from this parasite are internalized by the host cell, resulting in modulation of host:parasite adherence and

Significance

Extracellular vesicles (EVs) produced by one cell and internalized by a different cell are widely used for cellular communication and protein and RNA exchange between cells. Cancer metabolism and immune and neuronal responses are modulated by mammalian EVs. The uptake of parasite EVs by host cells also modifies host:pathogen interactions. Our research identifies surface components of both the host cell and EVs produced by the parasite *Trichomonas vaginalis* and defines cellular mechanisms critical for EV internalization and cross-talk between different cell types. Our findings reveal mechanisms that a pathogen can use to communicate with its host. This study is also instructive in guiding medical therapeutics aimed at exploiting EVs for drug and vaccine delivery.

Author contributions: A.K.R. and P.J.J. designed research; A.K.R. performed research; P.J.J. contributed new reagents/analytic tools; A.K.R. and P.J.J. analyzed data; and A.K.R. and P.J.J. wrote the paper.

Reviewers: A.H.B., University of Edinburgh; and S.L.H., University of Georgia.

The authors declare no competing interest.

See QnAs on page 21339.

[1]To whom correspondence may be addressed. Email: johnsonp@ucla.edu.

This article contains supporting information online at www.pnas.org/lookup/suppl/doi:10.1073/pnas.1912356116/-/DCSupplemental.

First published October 10, 2019.

host cell metabolism (14). Here, we examine both host cell and EV surface components involved in EV internalization and the mechanism that drives uptake. We utilized 2 biochemical assays: one that monitors host cell uptake of EVs by measuring membrane lipid fusion (the R18 assay) (Fig. 1*A*) and a second that measures EV soluble protein uptake (carboxyfluorescein succinimidyl diacetate ester [CFSE] assay) (Fig. 2*A*).

After determining that 10 μg EVs resulted in optimal detection of EV uptake, we labeled 10 μg *T. vaginalis* EVs from strain B7RC2 with either R18 or CFSE. After washing to remove unincorporated dye, labeled EVs were then incubated with Benign Prostatic Hyperplasia-1 (BPH-1) host cells at 37 °C for 30 min, the optimal temperature and time for EV uptake (*SI Appendix*, Fig. S1). Cells were then analyzed for R18 or CFSE fluorescence using a flow cytometer. Host cells incubated with EVs were found to have between ∼39- and ∼49-fold increase in fluorescence using the R18 or CFSE assay, respectively, compared with the host cell-only control (Figs. 1*B* and 2*B*). Fluorescently labeled hydrogenosomes (40, 41) were also included as a negative control, and very low fluorescence was detected (Figs. 1*B* and 2*B*), showing that uptake is EV specific. We also visualized the uptake of EVs and hydrogenosomes using fluorescence microscopy. As predicted, R18 or CFSE fluorescence was visible in host cells incubated with EVs, whereas only background levels of R18 or CFSE fluorescence were observed in host cells incubated with hydrogenosomes (Figs. 1*C* and 2*C*).

These results were confirmed quantitatively using spectrofluorimetry. Using fluorimetry, we also added detergent to induce 100% dequenching of R18-labeled EVs, which allowed us to calculate that ∼55% of EVs were internalized by host cells under our assay conditions of 37 °C and 30-min incubation (*SI Appendix*, Fig. S2).

Host Cell Heparan Sulfate Proteoglycans Mediate *T. vaginalis* EV Internalization. Limited analyses of the uptake of mammalian EVs by mammalian cells indicate a role for host cell glycans in the internalization of EVs (37, 42). We, therefore, tested whether host cell glycans affected *T. vaginalis* EV uptake by utilizing CHO

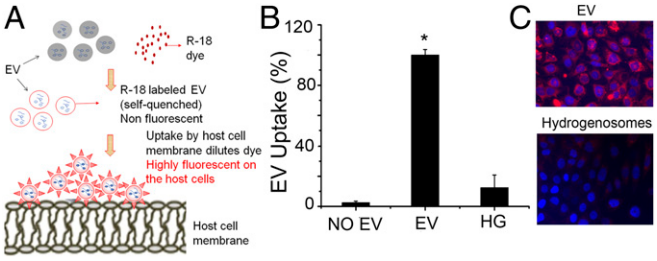

Fig. 1. EV uptake measured using a lipid-based assay. (*A*) To examine the uptake of EVs into host cells, we used a fluorescence dequenching assay utilizing EVs labeled with the lipophilic dye Octadecyl Rhodamine B Chloride (R18). The uptake of labeled R18 EVs by host cells results in a decreased R18 membrane surface density and dequenching, resulting in fluorescence proportional to EV uptake. R18-labeled EVs are shown with a red membrane, and red triangles depict the fluorescence that results when R18 is diluted in the host cell membrane during uptake. (*B*) *T. vaginalis* EVs or hydrogenosomes (HGs) were labeled with R18 dye, unbound dye was removed by gel filtration, and labeled EVs or HGs were incubated with BPH-1 cells for 30 min. Data shown represent the mean ± SD from 3 independent experiments, each performed in triplicate. Mean fluorescence without EV treatment =6,990.2 arbitrary units (AU), mean fluorescence with EVs treatment =271,829 AU, and mean fluorescence with HGs treatment =34,180.2 AU. The maximal fluorescence after incubating with labeled EVs was arbitrarily set at 100%. $*P < 0.05$. (*C*) EV uptake was visualized using fluorescence microscopy by incubating BPH-1 cells with R18-labeled EVs or HGs. Blue is DAPI stain, and red is R18 dye. These images are representative of 5 images viewed under similar condition.

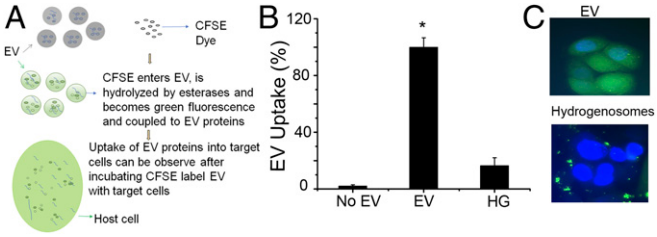

Fig. 2. EV uptake measured using a protein-based assay. (*A*) CFSE is a membrane-permeable dye that enters EVs and is hydrolyzed by esterases. Activated CFSE coupled to amines on EV proteins fluoresces green, allowing the tracking of EV proteins internalized into target cells. (*B*) *T. vaginalis* EVs or hydrogenosomes (HGs) were labeled with CFSE dye, unbound dye was removed by ultracentrifugation, and labeled EVs or HGs were incubated with BPH-1 cells for 30 min. Data shown represent the mean ± SD from 3 independent experiments, each performed in triplicate. Mean fluorescence without EV treatment =1,206.94 arbitrary units (AU), mean fluorescence with EVs treatment =58,634.24 AU, and mean fluorescence with HGs treatment =9,667.36 AU. The maximal fluorescence after incubating with labeled EVs was arbitrarily set at 100%. $*P < 0.05$. (*C*) EV uptake was visualized using fluorescence microscopy by incubating BPH-1 cells with CFSE-labeled EVs or HGs. Blue is DAPI stain, and green is CFSE dye. The images are representative of 5 images viewed under similar conditions. In all experiments, the maximal fluorescence after incubating with labeled EVs was arbitrarily set at 100%.

cell lines that either lack xylosyltransferase and do not produce any glycosaminoglycans (GAGs; ΔGAG; cell line pgsA-745) or lack both *N*-acetylglucosaminyltransferase and glucuronyltransferase activities required for heparan sulfate (HS) synthesis (ΔHS; cell line pgsD-677) (43, 44); pgsD-677 cells do not produce HS and produce 3 times more chondroitin sulfate than wild-type cells. The parent wild-type K1 CHO cell line was used as a positive control. As shown in Fig. 3*A*, the loss of all host cell surface GAGs reduced EV uptake by ∼70%, and the loss of just HS reduced uptake by ∼45%. To confirm a role for heparan sulfate proteoglycans (HSPGs) in EV uptake, we performed HS competition assays, adding exogenous HS to EV uptake assays using BPH-1 cells. We found a decrease in EV uptake with increasing HS concentrations, with ∼65% decrease in EV uptake at 20 μg/mL HS (Fig. 3*B*). We also enzymatically removed HS from the host cell surface using 10 mU heparan lyase III and measured an ∼65% reduction in EV uptake after 30-min incubation (Fig. 3*C*). Together, these data establish an important role for GAGs and HSPGs in *T. vaginalis* EV uptake.

It is notable that the loss of all GAGS (ΔGAG; cell line pgsA-745) or loss of HS (ΔHS; cell line pgsD-677) does not completely block EV update, indicating that there are likely additional cell surface components capable of mediating *T. vaginalis* EV update by host cells. HS may also be an essential coreceptor that partners with a specific receptor yet to be defined. If HS on host cell HSPGs is found to act in absence of a specific receptor, this would suggest a broad tropism for human host cells capable of EV uptake not limited to epithelial cells, such as the BPH and CHO cells tested here.

We next tested whether the presence of Ca^{2+} affected binding of EVs to HS. As shown in Fig. 4 *A* and *B*, EVs were loaded on HS sepharaose in the presence or absence of Ca^{2+}. The percentage of EVs in the unbound fraction and the percentage eluted with 1 or 2 M NaCl were determined, demonstrating that EV–HS interaction is dependent on Ca^{2+}. We then tested whether EV uptake is Ca^{2+} dependent, and as predicted, uptake was significantly decreased in the absence of Ca^{2+} (Fig. 4*C*). Together, these results indicate that HS chains on host cell HSPGs mediate EV uptake in a charge- and density-dependent manner.

4-α-Glucanotransferases Containing Carbohydrate Binding Domains Are Abundant Proteins in the *T. vaginalis* EV Proteome. Given that host cell HSPGs were found to be involved in EV uptake, we

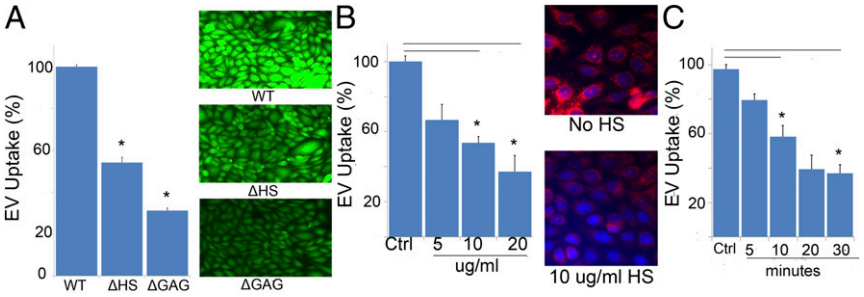

Fig. 3. Host cell proteoglycans mediate EV uptake. (*A*) Quantification of uptake of R18-labeled EVs incubated with the wild type (WT), HS deficient (ΔHS), and GAG deficient (ΔGAG) using flow cytometry (*Left*) and viewed by fluorescence microscopy (*Right*). These images are representative of 4 images viewed under similar condition. (*B*) Exogenous HS was added at the indicated micrograms per milliliter concentrations to EV uptake assays using BHP-1 cells, quantified using flow cytometry (*Left*), and viewed by fluorescence microscopy (*Right*). (*C*) Quantification of effect of enzymatic removal of HS from the host cell surface using 10 mU heparan lyase III incubated for the indicated minutes. Data shown represent the mean ± SD from 3 independent experiments, each performed in triplicate (*A* and *B*) and duplicate (*C*). Crtl, control. *$P < 0.05$.

analyzed the *T. vaginalis* EV proteome (14) for putative membrane proteins with carbohydrate binding domains. We found 3 highly abundant homologous proteins (TVAG_157940, TVAG_154680, and TVAG_222040) that share 88% amino acid identity and contain 2 N-terminal carbohydrate binding module domains (Carbohydrate-Binding Module 20 [CBM20] domains). These proteins are homologs of 4-α-glucanotransferases, which have been described in bacteria, plants, and several unicellular eukaryotes (45). The 4-α-glucanotransferases also contain C-terminal glycosyl hydrolase domains. Glucanotransferases have been shown to interact with large complex carbohydrates, and deletion of the CBM20 domains abolishes this interaction (45).

4-α-Glucanotransferase Binds HS and Competitively Inhibits EV Uptake. To test whether the interaction of the CBM20 domain(s) of the 4-α-glucantransferases with host cells affects EV uptake, we produced a 248-amino acid polypeptide that contains the CBM20 domains as a recombinant protein in *Escherichia coli*. We used the N-terminal domain of TVAG_157940, as this protein is the most abundant of the 3 glucanotransferases identified in the EV proteome (14). To directly measure the binding affinity of the CBM20 domains for HS, we used isothermal titration calorimetry (ITC) to measure the heat change associated with this interaction. The change in heat was then integrated to obtain thermodynamic parameters of binding. We found that injection of HS into a solution containing the polypeptide produced strong heat changes. With progressive injections, the heat signal decreased as the HS binding sites of the polypeptide became saturated. As shown in Fig. 5*A*, we calculated that this polypeptide binds HS with high affinity (K_d = 552 nM), whereas control bovine serum albumin (BSA) protein was measured to bind with a K_d = 4.44 mM.

Moreover, addition of the recombinant polypeptide in EV uptake reactions inhibited EV internalization ∼80% (Fig. 5*B*). These data define 4-α-glucanotransferases as EV ligands and indicate that the CBM20 carbohydrate binding domain binds to host cell HSPGs to mediate EV uptake. These analyses identify a surface protein(s) on *T. vaginalis* EVs that plays an important role in the internalization of the EVs. Here, we report on an EV ligand involved in the uptake of pathogen-derived or mammalian EVs.

***T. vaginalis* EVs Are Internalized by Clathrin-Independent Lipid Raft-Mediated Endocytosis.** Studies on the mechanism(s) of EV uptake are limited and have exclusively examined the internalization of mammalian EVs by mammalian cells (37). Inhibition of *T. vaginalis* EV uptake at 4 °C (*SI Appendix*, Fig. S1) indicates that internalization is an active process. Thus, we have examined whether internalization occurs via phagocytosis, micropinocytosis, clathrin-mediated endocytosis, or caveolae-dependent endocytosis using classic methods that utilize pharmacological drugs known to specifically inhibit these pathways (38, 46, 47).

To test whether EV uptake proceeds via clathrin-mediated endocytosis, well-defined inhibitors of this pathway were used in our EV uptake assays. As shown in Fig. 6, pretreatment of BPH-1 cells prior to addition of parasite EVs with these inhibitors only marginally affected uptake. Likewise, inhibitors that block phagocytosis and micropinocytosis have little effect on EV uptake.

In contrast, use of chemical reagents that inhibit caveolae-dependent endocytosis and disrupt lipid rafts dramatically reduced parasite EV uptake (Fig. 7*A*). Genistein and dynamin

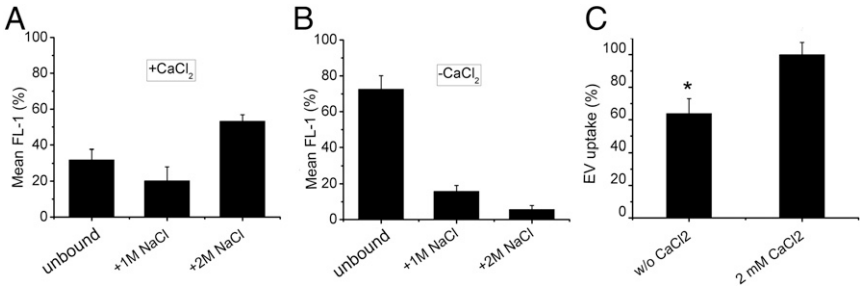

Fig. 4. Effects of $CaCl_2$ on EV uptake. (*A* and *B*) HS sepharose and R18-labeled EVs were incubated with (*A*) or without (*B*) 2 mM $CaCl_2$, and the fraction of EVs that did not bind in the absence of NaCl (unbound) or the presence of 1 or 2 M NaCl was quantified by fluorimetry-based assay. (*C*) EV uptake of R18-labeled EVs with or without 2 mM $CaCl_2$ was determine by flow cytometry. A significant decrease (*$P < 0.05$) in EV uptake was observed without $CaCl_2$. Data shown represent the mean ± SD from 3 independent experiments, each performed in triplicate.

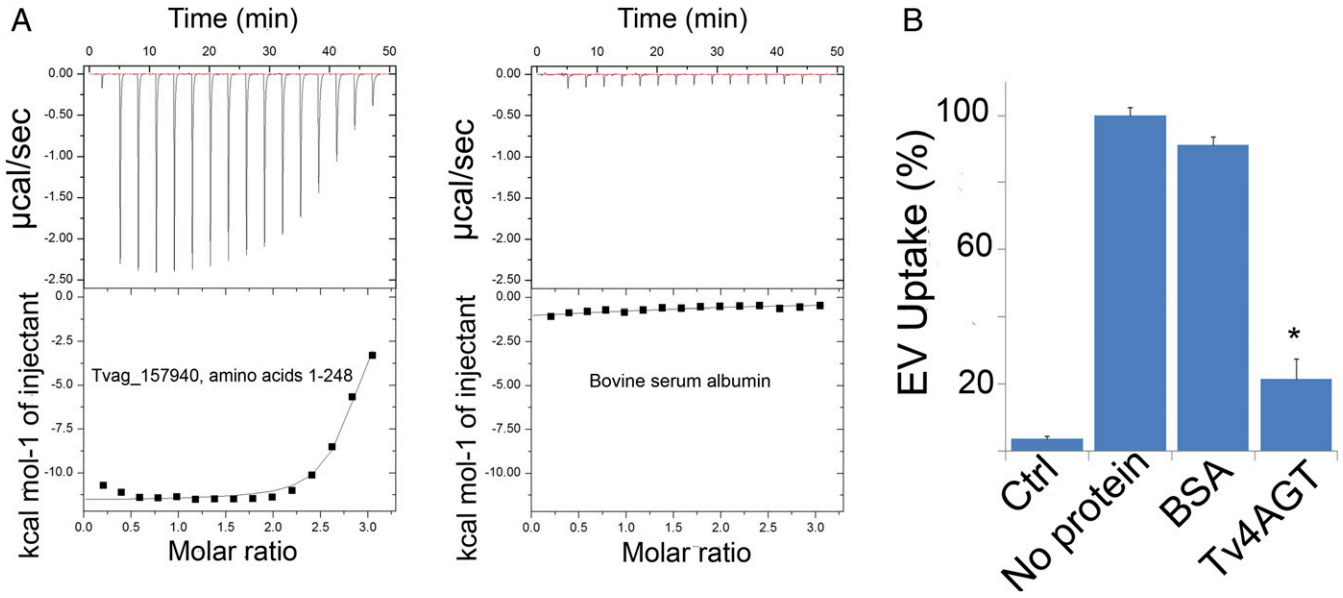

Fig. 5. The N-terminal fragment of 4-α-glucanotransferase binds HS and inhibits EV uptake. (*A*) ITC measurements of the binding of 4-α-glucanotransferase to HS; 1 mg/mL HS was added to equal concentrations (52 mM) of the N-terminal 248 amino acids of 4-α-glucanotransferase (TVAG_157940) or BSA, and the binding affinities were calculated using ITC at 25 °C. The raw titration data (*Upper*) and the integrated heat changes (*Lower*) are shown. Thermodynamic parameters were obtained to calculate K_d values. The dissociation constant (K_d) was determined from $1/K_a$. (*B*) The 248-amino acid polypeptide was added to EV uptake assays using BPH-1 cells. Either 3.5 µg of BSA or 3.5 µg of 4-α-glucanotransferase polypeptide (Tv4AGT) was incubated with the cells to examine the effect on EV uptake. The maximal fluorescence after incubating with labeled EVs with no added protein was set at 100%. Data shown represent the mean ± SD from 3 independent experiments, each performed in triplicate. Ctrl, control. *Significant decrease at $P < 0.05$.

inhibitory peptide, which inhibit lipid raft-mediated endocytosis (48, 49), blocked EV uptake by ∼90%. Filipin III, an inhibitor of lipid raft-dependent and caveolar endocytosis, also inhibited EVs uptake by ∼82%. To confirm the specificity of the drugs defined to target either clathrin-mediated endocytosis or caveolae-dependent endocytosis, we monitored endocytosis of transferrin (50) (the model protein for studying clathrin-mediated endocytosis) and cholera toxin B subunit (51) (a classical substrate for caveolae-dependent endocytosis). As predicted, we found that all drugs specifically targeted 1 of 2 pathways and not the other (*SI Appendix*, Figs. S3 and S4), allowing us to distinguish the endocytic pathways used to internalize *T. vaginalis* EVs.

As cholesterol is essential for maintenance of caveolae-enriched lipid rafts (52) and caveolae-dependent endocytosis is sensitive to cholesterol depletion (53), we tested whether the cholesterol depletion agent, methyl-β-cyclodextrin (MβCD), inhibited EV uptake. As shown in Fig. 7*B*, pretreatment of host cells with 50 mM MβCD blocked EV uptake by ∼90%. We confirmed that this effect was specific to depletion of cholesterol, as adding cholesterol back to the host cells restored uptake to ∼70%. Similar results were also obtained using fluorescence microscopy (*SI Appendix*, Fig. S5). These results show that EV uptake requires cholesterol, consistent with internalization by caveolae-dependent, lipid raft-mediated endocytosis.

Host Cell Caveolin-1 Mediates Lipid Raft-Dependent Endocytosis of EVs. Caveolin-1 plays a critical role in lipid raft-dependent endocytosis (54, 55). We, therefore, tested whether host cell caveolin-1 affects *T. vaginalis* EV uptake by utilizing human embryonic kidney 293 (HEK-293) cells where the endogenous level of caveolin-1 is very low (56). As shown in Fig. 8, EV uptake was reduced by ∼80% in HEK-293 cells compared with uptake by BPH-1 and K1 CHO cell lines.

To confirm a direct role of caveolin-1 in EV uptake, we transfected HEK-293 cells with a plasmid encoding caveolin-1 and then, selected for high levels of caveolin-1 expression. We found an ∼75% increase in EV uptake by HEK-293 cells overexpressing caveolin-1 compared with wild-type HEK-293 cells that express low levels of caveolin-1 (Fig. 8). Altogether, these results indicate that *T. vaginalis* EV uptake is mediated by lipid raft-dependent endocytosis in which host cell caveolin-1 plays a regulatory role.

Summary and Conclusions

We have developed assays to study the interface between parasite EVs and mammalian host cells and to quantify EV internalization by mammalian cells. Using these assays, we show that *T. vaginalis* EVs bind HSPGs present on the surface of host cells and that competition with HS or loss of HS from the host cell surface strongly inhibits EV uptake. These data indicate that HSPGs on host cells act as receptors in the first step of EV internalization. We also isolated and characterized an EV protein that binds HS and competes for EV internalization, thus identifying an EV ligand critical for EV uptake.

Utilizing well-defined methods, we have also shown that *T. vaginalis* EVs are internalized by mammalian cells via caveolae and lipid raft-dependent endocytosis, a demonstration of a role for caveolin-dependent lipid raft-mediated endocytosis in the uptake of EVs. Distinct EV uptake mechanisms might have evolved for *T. vaginalis* and mammalian EVs to prevent competition and interference of pathogen and host cell EVs at the site of infection. The little known about the mechanism of uptake of mammalian EVs by mammalian cells is consistent with mammalian EVs using different internalization mechanisms depending on EV origin and cell type. For example, pheochromocytoma cell-derived EVs enter host cells via clathrin-mediated endocytosis and micropinocytosis (38), whereas cancer cell-derived EVs are proposed to use HSPGs as internalizing receptors (39). EVs from different pathogens and different mammalian tissues or cancers likely use a variety of ligands, receptors, and internalization pathways given the physiological and evolutionary diversity of EVs and their target cells. Future analyses of the internalization of EVs from multiple organisms and tissue types will be necessary to fully understand the mechanisms involved in EV-mediated cell:cell communication.

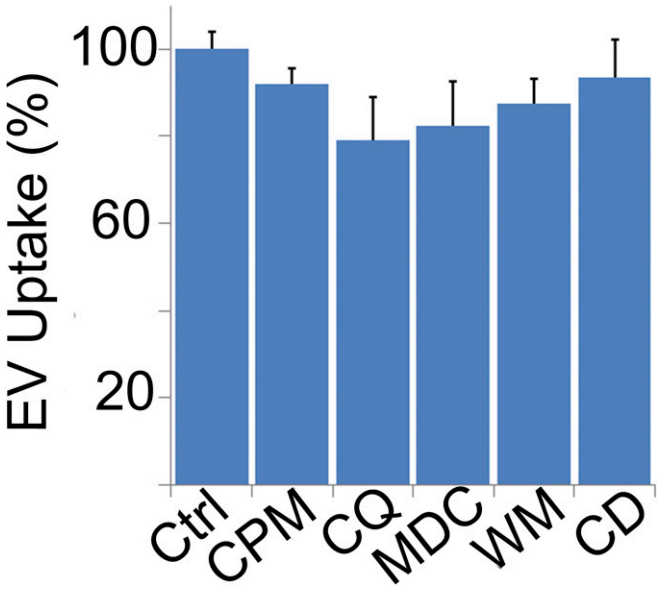

Fig. 6. EVs are not internalized via clathrin-mediated endocytosis or phagocytosis/micropinocytosis. BPH-1 cells were pretreated with known inhibitors of clathrin-mediated endocytosis or phagocytosis/micropinocytosis prior to addition of EV, and uptake was quantified by flow cytometry: no inhibitor (control [Ctrl]); clathrin-mediated endocytosis inhibitors: chlorpromazine (CPM), chloroquine (CQ), and monodansylcadeverine (MDC); and phagocytosis/micropinocytosis inhibitors: wortmannin (WM) and cytochalasin D (CD). The maximal fluorescence after incubating with labeled EVs in the absence of inhibitor (Ctrl) was set at 100%. Data shown represent the mean ± SD from 3 independent experiments, each performed in triplicate. No statistically significant difference was observed. Fluorescence microscopy confirmed these results.

These studies further our understanding of how EVs are internalized by target cells to allow cross-talk between different cell types. Our findings also describe mechanisms used to drive host:pathogen interactions. A better understanding of pathogen EVs will reveal additional physiological roles of these vesicles in infection and provide valuable insight to guide the use of EVs in future therapeutic and vaccination strategies.

Materials and Methods

Cell Cultures and Generation of Stable Cell Lines. *T. vaginalis* strain B7RC2 (American Type Culture Collection [ATCC] 50167) and the BPH-1 epithelial cell line were grown as previously described in refs. 57 and 58, respectively. K1 CHO cells were obtained from ATCC (CCL-61). CHO mutants A745 (23a1) and D677 (HS GAG-defective) cells (42, 43) were a gift from Jeffrey D. Esko, University of California San Diego, La Jolla, CA. CHO cells were cultured in F12 medium (Life Technologies, Inc.) supplemented with 10% fetal bovine serum (FBS) and 1% penicillin/streptomycin (Invitrogen) at 37 °C with 5% CO_2. HEK-293 cells were cultured in Dulbecco's modified Eagle medium with 10% FBS, 1% penicillin/streptomycin, and 1% glutamine (Invitrogen). HEK-293 cells overexpressing caveolin-1 were obtained by transfecting HEK-293 cells at 50% confluency with 400 ng of mCherry-Caveolin-1 plasmid (Addgene plasmid 55008) following the protocol for Lipofectamine LTX with Plus reagent in 50% (vol/vol) Opti-MEM/media (Thermo Fisher). Cells were transfected in 6-well plates and cultured for a week with new media without lipofectamine and washed cells before using in EV uptake experiments.

EV Isolation and Fluorescence Labeling. *T. vaginalis* was grown to a density of 1×10^6 cells per milliliter in Trypticase–yeast extract–maltose media, and EVs were isolated as previously described (14). Concentration of EV protein was quantified by using the Pierce BCA Kit (Thermo Scientific). EVs were subjected to Octadecyl Rhodamine B Chloride (R18; Molecular Probes) and Exo-Green CFSE (System Bioscience) fluorescent labeling according to the manufacture's recommendations followed by extensive washing to remove residual dye as described previously (59, 60). Briefly, 10 μg/mL EVs were labeled with 1 μL of an ethanolic solution of the fluorescent lipophilic probe R18 for 30 min at room temperature in 1 mL of 2-(*N*-morpholino) ethanesulfonic acid (MES) buffer (10 mM MES, pH 7.4, 145 mM NaCl, 5 mM KCl). The unbound R18 was removed by using a Sephadex G-75 column (20 × 1 cm) equilibrated with saline buffer; 10 μg/mL EVs were labeled with 5 μL Exo-Green dye for 10 min at 37 °C in 500 μL of phosphate-buffered saline (PBS) buffer. The unincorporated Exo-Green dye was removed by 100,000 × *g* for 60 min. Labeled EVs were resuspended in PBS at pH 7.4 and stored at −20 °C.

Internalization of EVs by BPH-1 or CHO Cells. Mammalian cells (10^6) were detached from culture plates using Cell Dissociation Buffer Enzyme-Free PBS based (Life Technologies), and cells were washed and resuspended in 1× PBS (pH 7.4). Titration of EVs using 2.5 to 25 μg/mL EVs in a 30-min reaction showed saturation of uptake at 10 μg/mL. Therefore, 10 μg/mL R18-labeled EVs or 10 μg/mL CFSE-labeled EVs were incubated with 5×10^4 BPH-1 or CHO cells in 400 μL for 30 min. Mammalian cells were analyzed for R18 or green fluorescent protein wavelength fluorescence using the LSRFortessa (BD Biosciences) flow cytometer. BPH-1–only reactions were used as a negative control. The percentage EV uptake was measured as the difference with respect to initial fluorescence of host cells and expressed as percentage of maximal fluorescence after incubating with the labeled EV. In all experiments, the maximal fluorescence after incubating with labeled EVs was arbitrarily set at 100%.

For fluorescence microscopy, BPH-1 or CHO cells were grown to 80% confluency on coverslips and washed with serum free media extensively before adding the EVs; 10 μg/mL fluorescently labeled EVs or hydrogenosomes were added to the cells and incubated for 2 h at 37 °C. Cells were washed twice with PBS (pH 7.4) to remove surface-associated EVs and were then mounted with ProLong Gold Antifade reagent with 4′,6-diamidino-2-phenylindole (DAPI) (Invitrogen). Fluorescence was imaged using an Axio ImagerZ1 fluorescent microscope (Zeiss) and analyzed using Zen Blue software (Zeiss).

EV Binding to HS. HS sepharose was washed with PBS buffer with or without 2 mM $CaCl_2$ by centrifugation at 500 × *g* for 10 min at 4 °C. R18-labeled EVs (10 μg/mL) were added to the HS sepharose, and mixtures were incubated at 4 °C for 30 min. Binding fractions of EV were eluted by PBS containing 1 and 2 M NaCl. Total EVs fluorescence signals of washes and elutions were recorded and calculated using QuantaMaster spectrofluorimeter (Horiba) and Origin Software.

Treatment with Heparinase III and Competition with HS. To digest cell surface HS, host cells were treated with 10 mU heparinase III (New England Biolabs) for 30 min at 37 °C followed by extensive washing and EV uptake analysis by flow cytometry (as described above). HS was used to compete in EV uptake assays by incubating BPH-1 cells with R18 EVs (10 μg/mL) for 30 min in the absence and in the presence of HS (5, 10, and 20 μg/mL) and then, analyzing for EV uptake by flow cytometry.

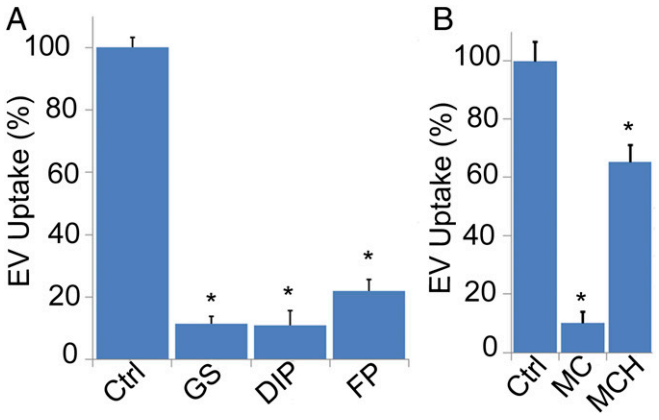

Fig. 7. Effect on EV uptake by inhibitors that block caveolae-dependent endocytosis and disrupt lipid rafts by cholesterol depletion. (*A*) Inhibitors added were no inhibitor (control [Ctrl]), genistein (GS), dynamin inhibitor peptide (DIP), and filipin (FP). The maximal fluorescence after incubating with labeled EVs in the absence of treatment (Ctrl) was set at 100%. Data shown represent the mean ± SD from 3 independent experiments, each performed in triplicate. *Significant decrease at $P < 0.05$ vs. Ctrl. (*B*) Effect of cholesterol depletion and add back: no treatment (Ctrl), MβCD (MC), and MβCD treatment plus cholesterol added back (MCH). Data shown represent the mean ± SD from 3 independent experiments, each performed in duplicate. *$P < 0.05$.

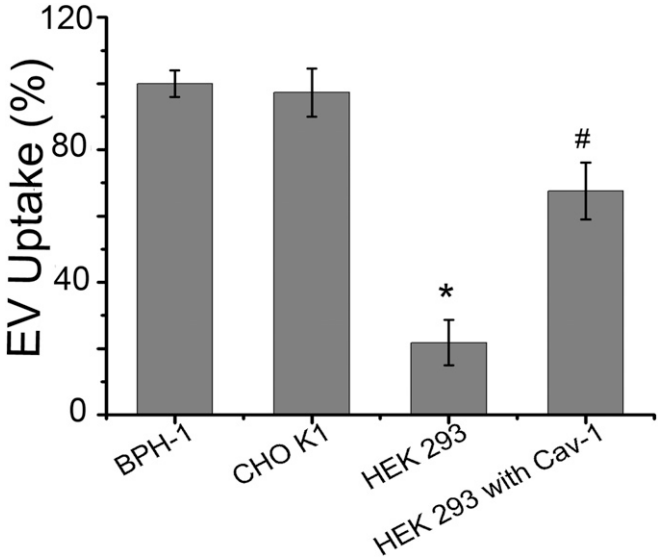

Fig. 8. Host cell caveolin-1–mediated lipid raft-dependent EV uptake. Quantification of R18-labeled EV uptake by BPH-1, K1 CHO, HEK-293 cells, and HEK-293 transfected with caveolin-1 using flow cytometry. The maximal fluorescence after incubating with labeled EVs with BPH-1 cells was set at 100%. Data are presented are the mean ± SD from 3 independent experiments, each performed in triplicate. A significant decrease (*$P < 0.05$) of uptake was observed for HEK-293 cells vs. BPH-1 or K1 CHO cells. Additionally, a significant increase ($^{\#}P < 0.005$) was observed upon overexpressing caveolin-1 in HEK-293 cells.

Recombinant Protein Generation and Purification. A DNA fragment encoding the first 248 amino acids of TVAG_157940 was generated using PCR, cloned into *E. coli* expression vector pET22b, and confirmed by DNA sequencing (61). *E. coli* BL21 was transformed, and protein expression was induced using isopropyl-β-D-thiogalactoside. The His-tagged protein was then purified by nickel-nitrilotriacetic acid agarose (Qiagen) affinity chromatography. Purity of the protein samples were confirmed by sodium dodecyl sulfate–polyacrylamide gel electrophoresis and Coomassie staining. Protein concentration was measured by monitoring absorbance at 280 nm on the basis of theoretically calculated molar extinction coefficient values obtained from the analysis of the amino acid sequences of the protein construct.

Isothermal Titration Calorimetry. ITC experiments were carried out at 25 °C using an iTC200 instrument (MicroCal/GE Healthcare). Isothermal titration reference cell was filled with sample buffer (10 mM Tris·HCl, pH 7.5), and proteins solutions (52 mM) were placed in the sample cell and then, titrated with HS (1 mg/mL) loaded in the syringe. The instrument settings were as follows: reference power, 10 μcal s^{-1}; initial delay, 300 s; stirring speed, 750 rpm; spacing, 180 s; injection, 0.2 μL (first injection) or 2 μL (subsequent injections); and low-feedback mode. No change in enthalpy was detected in control experiment (involving injecting HS in the BSA solutions). Raw data were collected and integrated using Origin 7 software. The dissociation constant (K_d) was determined from $1/K_a$ (K_a = binding constant).

Use of Inhibitors in EV Uptake Assay. BPH-1 cells were treated with chlorpromazine (50 μg/mL), chloroquine (150 μM), monodansylcadeverine (100 μM), wortmannin (100 nM), or cytochalasin D (5 μg/mL) in Roswell Park Memorial Institute (RPMI) culture medium for 30 min at 37 °C to test the effect on nonlipid raft-dependent EV internalization. Subsequently, R18-labeled EVs were coincubated with inhibitor-treated BPH-1 cells for 30 min, and EV uptake was analyzed by flow cytometry and fluorescence microscopy as described above.

To examine the effect on lipid raft-mediated uptake of EVs, BPH-1 cells were pretreated with Genistein (200 μM), dynamin inhibitor peptide (50 μM), or filipin (5 μg/mL) for 30 min at 37 °C. Cells were then incubated with R18-labeled EVs, and uptake was measured by flow cytometry and fluorescence microscopy as described above.

To test the effect of cholesterol on EVs uptake, cells were treated for 1 h at 37 °C in RPMI with 25 mM MβCD to deplete membrane cholesterol or with cholesterol-saturated MβCD to increase membrane cholesterol. Cholesterol-modifying medium was removed by washing with RPMI, and cells were assayed for uptake of R18-labeled EVs.

Uptake of Cholera Toxin B Subunit and Transferrin. To confirm the known effects of endocytosis inhibitors on the binding and uptake of cholera toxin B subunit and transferrin, pretreated cells were incubated with Alexa Fluor 594 conjugates of cholera toxin subunit B (1 mg/mL) or fluorescein conjugate of human transferrin (25 μg/mL) for 30 min. Cells were then analyzed using flow cytometry and fluorescence microscopy as described previously.

Statistical Analysis. Imaging experiments were performed in duplicate or triplicate in at least 3 independent experiments. Results in flow cytometry, HS binding, and fluorimetry experiments are the mean ± SD from 3 independent experiments. Graphs were made and statistical analyses were performed using Microsoft Excel 2010. Two-sample *t* tests were used to determine significance; a *P* value of <0.05 was considered significant.

ACKNOWLEDGMENTS. We thank Dr. Jeffrey D. Esko for the CHO cells. We thank all members of the laboratory of P.J.J. for valuable discussions and Dr. Frances Mercer, Dr. Katherine Muratore, Dr. Azeez Aranmolate, Brenda Molgora, and Fitz Gerald Diala for helpful comments on the manuscript. This work was supported by NIH Grants R01 AI103182 (to P.J.J.) and R21/R33 AI119721 (to P.J.J.).

1. A. C. Gerbase, J. T. Rowley, D. H. Heymann, S. F. Berkley, P. Piot, Global prevalence and incidence estimates of selected curable STDs. *Sex. Transm. Infect.* **74** (suppl. 1), S12–S16 (1998).
2. C. B. Menezes, A. P. Frasson, T. Tasca, Trichomoniasis - are we giving the deserved attention to the most common non-viral sexually transmitted disease worldwide? *Microb. Cell* **3**, 404–419 (2016).
3. R. P. Hirt, J. Sherrard, Trichomonas vaginalis origins, molecular pathobiology and clinical considerations. *Curr. Opin. Infect. Dis.* **28**, 72–79 (2015).
4. A. C. Seña *et al*., Trichomonas vaginalis infection in male sexual partners: Implications for diagnosis, treatment, and prevention. *Clin. Infect. Dis.* **44**, 13–22 (2007).
5. P. Kissinger *et al*., Trichomonas vaginalis treatment reduces vaginal HIV-1 shedding. *Sex. Transm. Dis.* **36**, 11–16 (2009).
6. R. S. McClelland *et al*., Infection with Trichomonas vaginalis increases the risk of HIV-1 acquisition. *J. Infect. Dis.* **195**, 698–702 (2007).
7. S. Gander, V. Scholten, I. Osswald, M. Sutton, R. van Wylick, Cervical dysplasia and associated risk factors in a juvenile detainee population. *J. Pediatr. Adolesc. Gynecol.* **22**, 351–355 (2009).
8. J. R. Stark *et al*., Prospective study of Trichomonas vaginalis infection and prostate cancer incidence and mortality: Physicians' Health Study. *J. Natl. Cancer Inst.* **101**, 1406–1411 (2009).
9. S. Sutcliffe, Sexually transmitted infections and risk of prostate cancer: Review of historical and emerging hypotheses. *Future Oncol.* **6**, 1289–1311 (2010).
10. C. M. Ryan, N. de Miguel, P. J. Johnson, Trichomonas vaginalis: Current understanding of host-parasite interactions. *Essays Biochem.* **51**, 161–175 (2011).
11. D. Leitsch, Recent advances in the Trichomonas vaginalis field. *F1000Res.* **5**, F1000 (2016).
12. P. Kissinger, Trichomonas vaginalis: A review of epidemiologic, clinical and treatment issues. *BMC Infect. Dis.* **15**, 307 (2015).
13. F. Mercer, P. J. Johnson, Trichomonas vaginalis: Pathogenesis, symbiont interactions, and host cell immune responses. *Trends Parasitol.* **34**, 683–693 (2018).
14. O. Twu *et al*., Trichomonas vaginalis exosomes deliver cargo to host cells and mediate host:parasite interactions. *PLoS Pathog.* **9**, e1003482 (2013).
15. O. Twu, P. J. Johnson, Parasite extracellular vesicles: Mediators of intercellular communication. *PLoS Pathog.* **10**, e1004289 (2014).
16. S. Ressel, A. Rosca, K. Gordon, A. H. Buck, Extracellular RNA in viral-host interactions: Thinking outside the cell. *Wiley Interdiscip. Rev. RNA* **10**, e1535 (2019).
17. M. Marti, P. J. Johnson, Emerging roles for extracellular vesicles in parasitic infections. *Curr. Opin. Microbiol.* **32**, 66–70 (2016).
18. A. J. Szempruch, L. Dennison, R. Kieft, J. M. Harrington, S. L. Hajduk, Sending a message: Extracellular vesicles of pathogenic protozoan parasites. *Nat. Rev. Microbiol.* **14**, 669–675 (2016).
19. M. J. Cipriano, S. L. Hajduk, Drivers of persistent infection: Pathogen-induced extracellular vesicles. *Essays Biochem.* **62**, 135–147 (2018).
20. A. J. Szempruch *et al*., Extracellular vesicles from trypanosoma brucei mediate virulence factor transfer and cause host anemia. *Cell* **164**, 246–257 (2016).
21. N. Regev-Rudzki *et al*., Cell-cell communication between malaria-infected red blood cells via exosome-like vesicles. *Cell* **153**, 1120–1133 (2013).
22. K. A. Babatunde *et al*., Malaria infected red blood cells release small regulatory RNAs through extracellular vesicles. *Sci. Rep.* **8**, 884 (2018).
23. A. H. Buck *et al*., Exosomes secreted by nematode parasites transfer small RNAs to mammalian cells and modulate innate immunity. *Nat. Commun.* **5**, 5488 (2014).

24. G. Coakley *et al*., Extracellular vesicles from a helminth parasite suppress macrophage activation and constitute an effective vaccine for protective immunity. *Cell Rep.* **19**, 1545–1557 (2017).
25. S. Montaner *et al*., The role of extracellular vesicles in modulating the host immune response during parasitic infections. *Front. Immunol.* **5**, 433 (2014).
26. S. M. Pope, C. Lässer, Toxoplasma gondii infection of fibroblasts causes the production of exosome-like vesicles containing a unique array of mRNA and miRNA transcripts compared to serum starvation. *J. Extracell. Vesicles* **2**, 22484 (2013).
27. L. M. Olmos-Ortiz *et al*., Trichomonas vaginalis exosome-like vesicles modify the cytokine profile and reduce inflammation in parasite-infected mice. *Parasite Immunol.* **39**, e12426 (2017).
28. J. M. Silverman *et al*., An exosome-based secretion pathway is responsible for protein export from Leishmania and communication with macrophages. *J. Cell Sci.* **123**, 842–852 (2010).
29. J. M. Silverman, N. E. Reiner, Leishmania exosomes deliver preemptive strikes to create an environment permissive for early infection. *Front. Cell. Infect. Microbiol.* **1**, 26 (2012).
30. A. S. Azmi, B. Bao, F. H. Sarkar, Exosomes in cancer development, metastasis, and drug resistance: A comprehensive review. *Cancer Metastasis Rev.* **32**, 623–642 (2013).
31. Y. L. Tai, K. C. Chen, J. T. Hsieh, T. L. Shen, Exosomes in cancer development and clinical applications. *Cancer Sci.* **109**, 2364–2374 (2018).
32. C. Ciardiello *et al*., Focus on extracellular vesicles: New frontiers of cell-to-cell communication in cancer. *Int. J. Mol. Sci.* **17**, 175 (2016).
33. D. W. Greening, S. K. Gopal, R. Xu, R. J. Simpson, W. Chen, Exosomes and their roles in immune regulation and cancer. *Semin. Cell Dev. Biol.* **40**, 72–81 (2015).
34. P. D. Robbins, A. E. Morelli, Regulation of immune responses by extracellular vesicles. *Nat. Rev. Immunol.* **14**, 195–208 (2014).
35. L. Rajendran *et al*., Emerging roles of extracellular vesicles in the nervous system. *J. Neurosci.* **34**, 15482–15489 (2014).
36. S. Koniusz *et al*., Extracellular vesicles in physiology, pathology, and therapy of the immune and central nervous system, with focus on extracellular vesicles derived from mesenchymal stem cells as therapeutic tools. *Front. Cell Neurosci.* **10**, 109 (2016).
37. L. A. Mulcahy, R. C. Pink, D. R. Carter, Routes and mechanisms of extracellular vesicle uptake. *J. Extracell. Vesicles* **3**, 24641 (2014).
38. T. Tian *et al*., Exosome uptake through clathrin-mediated endocytosis and macropinocytosis and mediating miR-21 delivery. *J. Biol. Chem.* **289**, 22258–22267 (2014).
39. H. C. Christianson, K. J. Svensson, T. H. van Kuppevelt, J. P. Li, M. Belting, Cancer cell exosomes depend on cell-surface heparan sulfate proteoglycans for their internalization and functional activity. *Proc. Natl. Acad. Sci. U.S.A.* **110**, 17380–17385 (2013).
40. P. J. Bradley, C. J. Lahti, E. Plümper, P. J. Johnson, Targeting and translocation of proteins into the hydrogenosome of the protist Trichomonas: Similarities with mitochondrial protein import. *EMBO J.* **16**, 3484–3493 (1997).
41. E. T. Bui, P. J. Bradley, P. J. Johnson, A common evolutionary origin for mitochondria and hydrogenosomes. *Proc. Natl. Acad. Sci. U.S.A.* **93**, 9651–9656 (1996).
42. M. Yáñez-Mó *et al*., Biological properties of extracellular vesicles and their physiological functions. *J. Extracell. Vesicles* **4**, 27066 (2015).
43. X. M. van Wijk *et al*., Whole-genome sequencing of invasion-resistant cells identifies laminin α2 as a host factor for bacterial invasion. *MBio* **8**, e02128-16 (2017).
44. J. D. Esko *et al*., Inhibition of chondroitin and heparan sulfate biosynthesis in Chinese hamster ovary cell mutants defective in galactosyltransferase I. *J. Biol. Chem.* **262**, 12189–12195 (1987).
45. J. M. Steichen, R. V. Petty, T. D. Sharkey, Domain characterization of a 4-alpha-glucanotransferase essential for maltose metabolism in photosynthetic leaves. *J. Biol. Chem.* **283**, 20797–20804 (2008).
46. H. Costa Verdera, J. J. Gitz-Francois, R. M. Schiffelers, P. Vader, Cellular uptake of extracellular vesicles is mediated by clathrin-independent endocytosis and macropinocytosis. *J. Control. Release* **266**, 100–108 (2017).
47. C. Escrevente, S. Keller, P. Altevogt, J. Costa, Interaction and uptake of exosomes by ovarian cancer cells. *BMC Cancer* **11**, 108 (2011).
48. D. Vercauteren *et al*., The use of inhibitors to study endocytic pathways of gene carriers: Optimization and pitfalls. *Mol. Ther.* **18**, 561–569 (2010).
49. P. U. Le, I. R. Nabi, Distinct caveolae-mediated endocytic pathways target the Golgi apparatus and the endoplasmic reticulum. *J. Cell Sci.* **116**, 1059–1071 (2003).
50. K. M. Mayle, A. M. Le, D. T. Kamei, The intracellular trafficking pathway of transferrin. *Biochim. Biophys. Acta* **1820**, 264–281 (2012).
51. C. A. Day, A. K. Kenworthy, Functions of cholera toxin B-subunit as a raft cross-linker. *Essays Biochem.* **57**, 135–145 (2015).
52. J. R. Silvius, Role of cholesterol in lipid raft formation: Lessons from lipid model systems. *Biochim. Biophys. Acta* **1610**, 174–183 (2003).
53. M. R. Marwali, J. Rey-Ladino, L. Dreolini, D. Shaw, F. Takei, Membrane cholesterol regulates LFA-1 function and lipid raft heterogeneity. *Blood* **102**, 215–222 (2003).
54. P. Lajoie, I. R. Nabi, Regulation of raft-dependent endocytosis. *J. Cell Mol. Med.* **11**, 644–653 (2007).
55. I. R. Nabi, P. U. Le, Caveolae/raft-dependent endocytosis. *J. Cell Biol.* **161**, 673–677 (2003).
56. J. Wharton, T. Meshulam, G. Vallega, P. Pilch, Dissociation of insulin receptor expression and signaling from caveolin-1 expression. *J. Biol. Chem.* **280**, 13483–13486 (2005).
57. C. G. Clark, L. S. Diamond, Methods for cultivation of luminal parasitic protists of clinical importance. *Clin. Microbiol. Rev.* **15**, 329–341 (2002).
58. S. W. Hayward *et al*., Establishment and characterization of an immortalized but non-transformed human prostate epithelial cell line: BPH-1. *In Vitro Cell. Dev. Biol. Anim.* **31**, 14–24 (1995).
59. I. Parolini *et al*., Microenvironmental pH is a key factor for exosome traffic in tumor cells. *J. Biol. Chem.* **284**, 34211–34222 (2009).
60. A. Morales-Kastresana *et al*., Labeling extracellular vesicles for nanoscale flow cytometry. *Sci. Rep.* **7**, 1878 (2017).
61. S. N. Ho, H. D. Hunt, R. M. Horton, J. K. Pullen, L. R. Pease, Site-directed mutagenesis by overlap extension using the polymerase chain reaction. *Gene* **77**, 51–59 (1989).